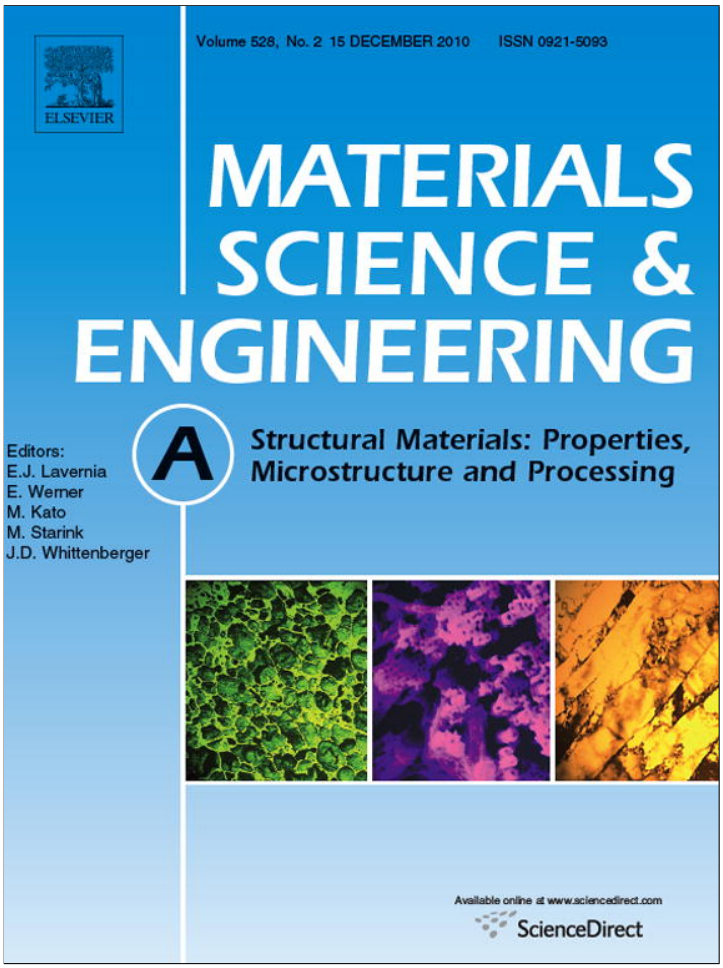

Materials Science and Engineering A 528 (2010) 745–750

Contents lists available at ScienceDirect

Materials Science and Engineering A

journal homepage: www.elsevier.com/locate/msea

Fatigue design factors for ECAPed materials

F. Djavanroodi*, M. Ebrahimi, B. Rajabifar, S. Akramizadeh

Department of Mechanical Engineering, Iran University of Science and Technology, Tehran, Iran

ARTICLE INFO

Article history:
Received 28 April 2010
Received in revised form
22 September 2010
Accepted 24 September 2010

Keywords:
ECAP
CG
UFG
Mechanical properties
Endurance limit
Fatigue design factor

ABSTRACT

Equal channel angular pressing (ECAP) was successfully performed on commercial pure aluminum, aluminum 6061 alloy and commercial pure copper by route B_C. Tensile and fatigue (under constant stress) tests shows a significant enhancement in mechanical properties consisting of hardness, yield strength, ultimate tensile strength and endurance limit, but the ductility of the alloys reduced with employing this process. Two fatigue design factors K_l and K_h has been suggested to co-related fatigue data from coarse grained (CG) to ultra-fine grained (UFG) materials.

1. Introduction

Severe plastic deformation (SPD) is an efficient method for producing ultra-fine grain (UFG) materials [1]. Various SPD techniques like equal channel angular pressing (ECAP) [2,3], cyclic extrusion compression (CEC) [4], high pressure torsion (HPT) [5], accumulative roll bounding (ARB) [6] and repetitive corrugation and straightening (RCS) [7] have been introduced for fabricating nano-structured materials. It is generally considered that nano-structured materials have high mechanical and super-plasticity properties [8]. Among all SPD methods the ECAP process has proved attractive and has been investigated because of no substantial change in the geometry of the sample. As can be seen in Fig. 1, a sample is pressed through a die with two intersecting channels equal in the cross-section with a die channel angle of ϕ and a corner angle of Ψ.

In the ECAP process there are four fundamental routes between each repetitive pressing as is shown in Fig. 2. These are: route A—that the sample is repetitively pressed without any rotation, route B_A—that the sample is rotated by 90° in alternative direction between each pass, route B_C—that the sample is rotated in the same sense by 90° and route C—that the sample is rotated by 180° between each pass [9]. These routes create different slip systems during the pressing operation so that various microstructure and mechanical properties can be achieved [10,11]. By using route B_C, a uniform distribution of the effective strain and a material with isotropic properties can be obtained using the ECAP process. Influences of die parameters and friction coefficient values on the effective strain distribution have been investigated by the authors [12].

Fatigue life of components consists of two stages: Stage one – high-cycle fatigue (HCF) – at relatively small strain amplitudes, the crack initiation stage dominates most of fatigue life. Stage two – low-cycle fatigue (LCF) – which is associated mostly with the crack propagation, which occurs at relatively large strains [13]. It is possible to distinguish quantitatively between the high and low cycle fatigue if the total life fatigue diagram is considered where the number of reversals to failure is plotted versus the total strain amplitude [14–18]. For the UFG materials produced by SPD techniques, a variety of increased or decreased fatigue properties in different researches are reported. However, most UGF materials produced by SPD techniques exhibit similar properties: their high cycle fatigue (HCF) strength is considerably higher than for coarse grain (CG) materials and their low cycle fatigue (LCF) is inferior in its ability to sustain cyclic loading in the LCF region [19]. The factors affecting the fatigue limit are: (a) chemical composition of the alloy, (b) type of dislocation slip, (c) grain size, (d) dislocation density and distribution, (e) texture, (f) residual stresses, (g) stress ratio, (h) mean stress, (i) frequency, (j) temperature, (k) environment, (l) specimen shape and dimensions, (m) surface conditions such as finishing and hardening/softening treatment of the surface layer [19–23]. The fatigue limit of pure f.c.c. metals (Cu and Al) with relatively high stacking fault energy and wavy slip behavior is not affected by the grain size [23]. The striking result of grain

* Corresponding author. Tel.: +9821 77240203.
E-mail address: javanroodi@iust.ac.ir (F. Djavanroodi).

0921-5093/$ – see front matter © 2010 Elsevier B.V. All rights reserved.
doi:10.1016/j.msea.2010.09.080

Table 1
Chemical composition of commercial pure aluminum, Al6061 and commercial pure copper.

Material	Composition						
Al1060	Al, base	Fe, 0.212	Si, 0.100	Cu, 0.015	Zr, 0.013	Ti, 0.009	Mg, 0.007
Al6061	Al, base	Mg, 0.800	Fe, 0.700	Si, 0.400	Zn, 0.250	Cu, 0.150	Ti, 0.150
Cu	Cu, base	P, 0.027	Sn, 0.005	Zn, 0.002			

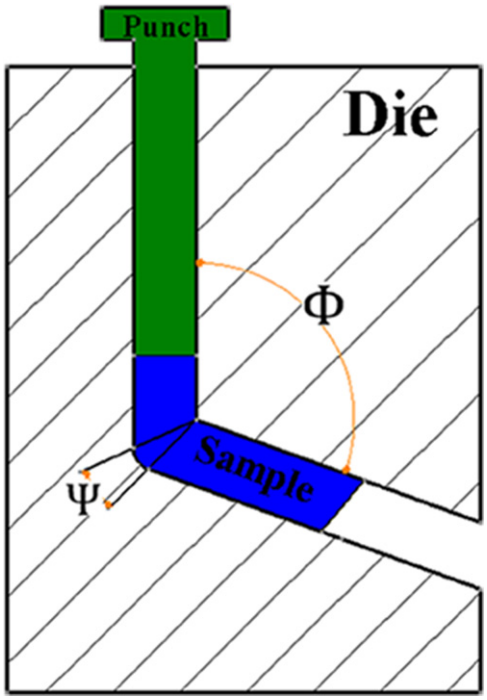

Fig. 1. The schematically diagram of ECAP die.

refinement down to submicrocrystalline scale is that these materials exhibit a prominent rise in their fatigue performance after ECAP.

The determination of endurance limits by fatigue testing is now routine, though a lengthy procedure. For preliminary design and failure analysis, a quick method of estimating endurance limit is needed. Also obtaining an endurance limit modifying factor which can be used to account for ECAPed process effect on the base material is very useful for designer when endurance limit of mechanical element are required. In this study, the ECAP process has been performed on three types of alloys (commercial pure aluminum, Al6061 and pure copper) by route B_C with the die channel angle of 90° and corner angle of 15°. Optical and scanning electron

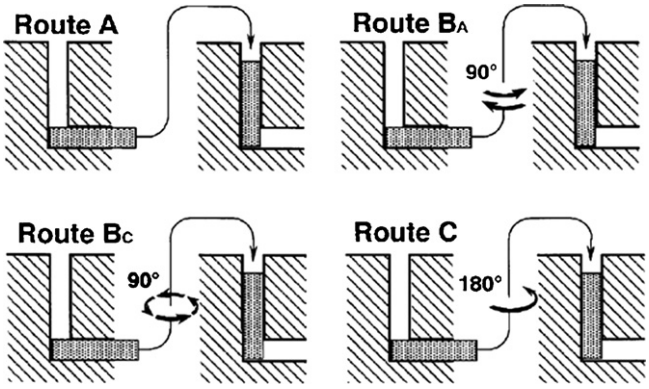

Fig. 2. Four fundamental routes in the ECAP process [9].

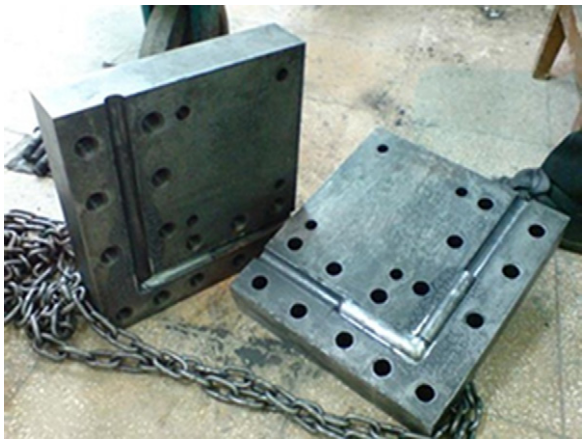

Fig. 3. ECAP die with $\Phi = 90°$ and $\Psi = 15°$ used for this study.

microscopy (SEM) has been used to evaluate and measure grain size of samples before and after pressing. Mechanical properties (hardness and tensile tests) and the *S–N* curve (fatigue strength–number of cycles) of base and the ECAPed materials are compared. Two fatigue design factors obtained from uniaxial test, K_l and $K_{h,}$ have been suggested to co-related fatigue data from coarse grained to ultra-fine grained materials.

2. Experimental procedures

The ECAP die was designed and manufactured with an internal angle of $\varphi = 90$ between the vertical and horizontal channels and a curvature angle of $\psi = 15$. Fig. 3 shows a general view of the ECAP die. Three types of alloys with the diameter of ~20 mm were used for this study: Al1060, Al6061 and pure Cu. The chemical compositions of these materials are shown in Table 1. The Al6061samples were solid-solutionized at 530 °C for about 2.5 h and then cooled to room temperature by slow cooling in the furnace (furnace cooled, FC). The pure Al samples were annealed at 360 °C for about 20 min and then cooled to room temperature by slow cooling in the furnace. The pure copper samples were also normalized at 500 °C for about 1 h and then cooled to room temperature in air. The purpose of these heat treatments was to increase the workability and ductility of the materials. The initial grain size measured after heat treatment and prior to ECAP was approximately 65, 110 and 120 μm for Al6061, Al1060 and pure Cu, respectively as shown in Table 2. The ECAP process was performed at room temperature with a ram speed of 1 mm s^{-1} and using samples lubricated with MoS_2. Route B_C was used for the ECAP process. Fig. 4 represents the shape of ECAPed samples. Hardness was measured on a plane perpendicular to the extrusion axis of the ECAP-processed materials,

Table 2
The grain size magnitudes for initial and final passes in Al1060, Al6061 and pure copper.

	Initial (mm)	ECAPed (nm)
Al1060	110	710
Al6061	65	590
Pure Cu	120	600

Fig. 4. The shape of ECAPed samples after 4 passes: left Al, middle Al6061 and right Cu.

according to ASTM E10-04. The hardness measurement was preformed at 3 different points, the center of the samples (where more homogeny of the strain was expected) on the surfaces of the cross section and the average was reported as the hardness of the surface. Tensile test specimens were machined from the center of the billet according to ASTM B557M. ECAPed samples were machined with their longitudinal axes parallel to the pressing axis. Tensile tests were carried out at room temperature with an initial strain rate of $2e{-}3\ S^{-1}$. The tensile testing machine was controlled under constant crosshead speed condition. Fatigue tests were carried out under a load control mode at a frequency of 74 Hz. The diameters of the fatigue samples were 8 mm and tests were performed under the fully reversed loading condition $R = -1$ where R is the ratio of the minimum stress to maximum stress for a cycle stress according to ASTM E466. For comparison purposes, tensile and fatigue tests were also carried out on the as-received materials. To verify refining of the grains, optical microscopy for initial samples and SEM for ECAPed samples were applied to measure the grain size of materials.

3. Results and discussion

3.1. Hardness and tensile strength enhancement

The measured Vickers hardness of the materials versus the number of the passes for pure Al, Al6061 and pure Cu on the plane perpendicular to the longitudinal axis of the ECAPed samples are shown in Fig. 5. As can be observed for each alloy, the magnitude of the hardness of all materials dramatically after a single pass of ECAP, but the rate of the hardness decreases as the number of passes increases for each curve. For example, in pure aluminum, an increase of approximately 175% is observed at the magnitude of the hardness after the first pass whereas only a 15% increase is seen at subsequent passes. The maximum hardness values for pure Al, Al6061 and pure Cu are ≈60 HV, ≈69 HB and ≈155 HB respectively. The effect of the increasing hardness magnitude and strength of the materials in the ECAP process were previously studied [24,25] and can be summarized as follows. As known, in each material, there are some dislocations which are uniformly distributed and display no specific network [26]. Also, by annealing samples before the ECAP operation, the distribution of dislocations becomes uniform and a high homogenous and isotropic material is achieved. With the starting process a sample subjected to intensive plastic deformation and dislocations started to move to the cell boundaries. On the other hand, the density of the dislocations upon imposing strain to the sample will increase gradually resulting in the formation of low angle boundaries (LAB) inside of the grain. By increasing the number of the passes, the LABs may progressively be transformed into high angle boundaries (HAB). So it can be said that sub-grains transform to new submicron or nanometer grains and new sub-grains are nearly free of dislocations in the interior [27]. It is also apparent from Fig. 5 that for pure Al (≈50 HV) and Cu (≈140 HB) after the second pass the hardness remains almost the same in the subsequent passes until the maximum number of 8 passes, whereas hardness for the Al6061 alloy increase in each additional pass up to a maximum value of ≈69 HB after 4 passes. For these two materials high dislocations density under a fixed applied load is achieved due to high stacking fault energy, a high strain hardening rate and a rapid recovery rate. Also, a short period of time to reach a straining saturation is required for these two materials because the only hardening mechanism exists in pure Al and Cu is dislocation hardening. By contrast, the Al6061 alloy has a lower stacking fault energy, a lower stain hardening rate, a relatively low rate of recovery and, in addition, the alloying elements play a role in providing barriers, in the form of precipitates, for dislocation movement. Therefore, alloy exhibits a relatively long region of strain hardening [28].

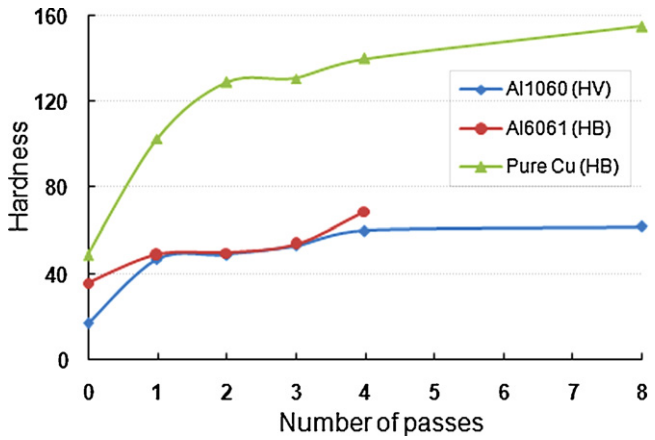

Fig. 5. Hardness versus the number of the passes for Al, Al6061 and Cu.

To validate the reduction of grain size, both un-ECAPed samples and ECAPed samples grain size were measured. Table 2 presents the average grain sizes before and after the ECAP process. As an example, the SEM microstructure of commercial pure copper after four pass ECAP is shown in Fig. 6.

3.2. Tensile strength and ductility changes

Table 3 shows the magnitudes of yield strength (σ_{yp}), ultimate tensile strength(σ_{UTS}), elongation (δ) and endurance limit of three alloys: pure Al, Al6061 and pure copper which were obtained from tensile and fatigue tests. As can be seen, significant changes in the magnitudes are obtained for the first pass and then gradual changes are observed for subsequent passes. The ECAP process has a negative effect on the ductility of the material. The reduction on elongation for alloys tested is shown in Table 3. For pure aluminum, Al6061 and pure copper a reduction in ductility of 60%, 45% and 80% has been measured after the ECAP process respectively. It is apparent that the magnitude of the elongation is reduced after the first pass but there are no substantial changes in its value in subsequent passes. As an example, stress–strain curves of pure Al before and after ECAP process are shown in Fig. 7.

3.3. Fatigue properties enhancement

S–N curves for both UFG and CG alloys are shown in Fig. 8. In this figure, the data are compared with earlier work of Estrin and Vinogradov [19] on pure aluminum, Chung et al. [22] on Al6061, Xu et al. [20] and Goto et al. [21] on copper. It is evident that the fatigue

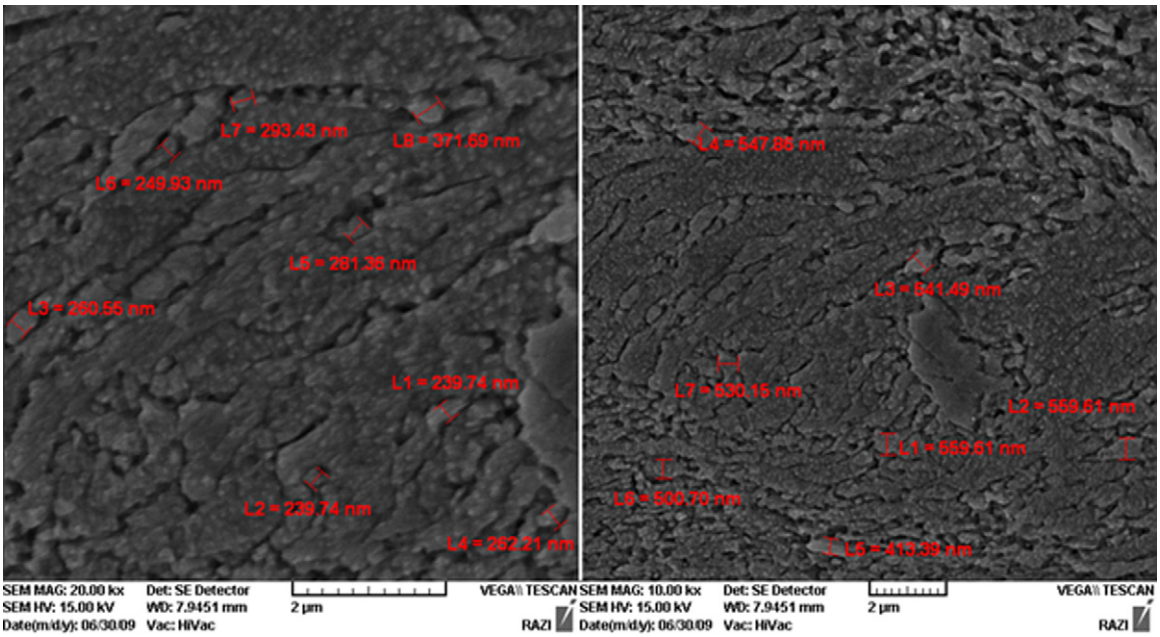

Fig. 6. The SEM microstructure of commercial pure copper after four passes by route B_C.

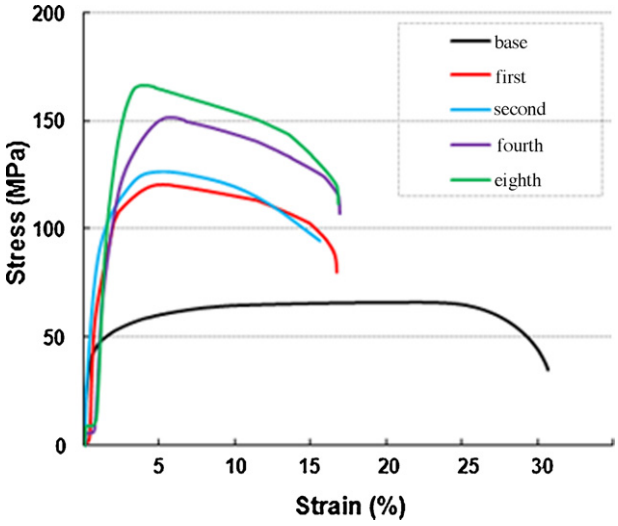

Fig. 7. The stress-strain curves of un-ECAP and ECAPed commercial pure Al.

lives of UFG samples were markedly longer than CG samples for all stress amplitudes. The life times of UFG the number of cycles to fracture increased continuously with decreasing stress amplitude in the whole interval studied. At applied stresses, the ECAP samples had an obvious advantage due to their higher yield strength. Compared with CG alloys, the *S–N* curve of UFG alloys was shifted to higher stress amplitudes. The endurance limits are defined on the basis of $\sim 10^6$ cycles are (21, 55), (55, 115) and (68, 197) in CG and UFG pure Al, Al6061 and pure Cu, respectively. These magnitudes of endurance limit show an enhancement of about 160% in pure Al, 110% in Al6061 and 190% in pure Cu. The result of grain refinement shows that Al and copper, which are wavy-slip materials (f.c.c.), exhibit a prominent rise in their fatigue performance after ECAP [23]. The effect of grain refinement on fatigue in terms of relative contribution of crack nucleation and crack growth rate are discussed in [29,30]. It is argued that grain refinement usually results in a greater resistance to crack initiation and faster crack propagation which is also in agreement with a review by Suresh [31]. The higher yield stress in the ECAP material prevents macroscopic plastic deformation at the beginning of load controlled cycling in contrast to the low-strength initial material. This, in turn, increases

Table 3
Mechanical and fatigue properties of pure Al, Al6061 and pure Cu before and after ECAP process.

Material	Steps	σ_{yp} (MPa)	σ_{UTS} (MPa)	δ (%)	Endurance limit (MPa)
Pure Al	Base	36	62	31	21
	First	75	121	15	–
	Second	76	124	14	–
	Third	121	145	14	–
	Fourth	125	152	13	–
	Eighth	127	167	14	55
Al6061	Base	87	122	23	55
	First	219	233	15	–
	Second	231	253	14	–
	Third	232	257	14	–
	Fourth	256	270	13	115
Pure Cu	Base	111	214	47	68
	First	280	395	15	–
	Second	357	417	15	–
	Third	358	451	11	–
	Fourth	428	481	10	197

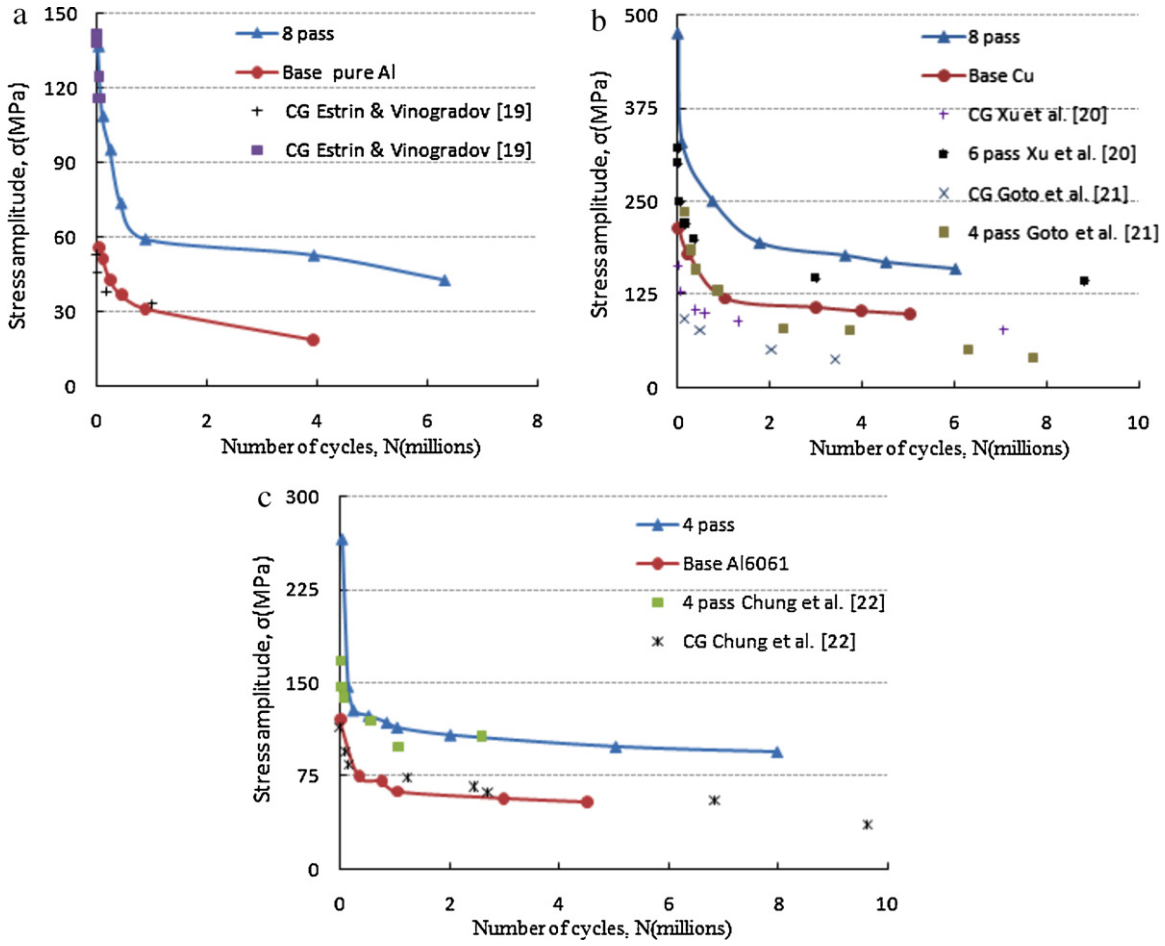

Fig. 8. *S–N* diagram of un-ECAP and ECAP alloys: (a) pure Al, (b) Cu, (c) Al6061.

the incubation period for crack nucleation and the total fatigue life in fine-grained material at high stresses.

3.3.1. Fatigue—limit modifying factors

The determination of endurance limits by fatigue testing is a lengthy procedure. For preliminary design and failure analysis, a quick method of estimating endurance limit is quite useful. Two factors which has been obtained from uniaxial tension test has been proposed to correlate the endurance limit S_e UFG materials with endurance limit S'_e of the CG materials.

At high strain amplitudes corresponding to short fatigue lives, the plastic strain component is prevalent in the total applied strain and the fatigue life is determined primarily by ductility. On the other hand at long fatigue lives, the elastic strain amplitude is more significant and fatigue life is dictated by the fracture strength, hence the endurance limit increases with tensile strength [31].

The endurance limit S_e of UFG materials may be considerably larger than the endurance limit S'_e of the CG materials. This difference may be explained by a variety of factors, each of which accounts for separate effects. Using this idea, and only considering the effect of increased strength, we may write:

$$S_e = K_h S'_e \qquad where\, K_h = \frac{(\sigma_{UTS})_{ECAP}}{(\sigma_{UTS})_{UN-ECAP}} \tag{1}$$

For the low cycle fatigue (LCF) at 1000 cycles, the Fatigue strength:

$$S = K_l S' \qquad where\, K_l = \frac{(\delta)_{UN-ECAP}}{(\delta)_{ECAP}} \tag{2}$$

Table 4 represented the magnitudes of K_h and K_l for pure aluminum, Al6061 and pure copper. The calculated endurance limit (Eq. (1)) for present work and number of earlier work of Goto et al. [21], Han et al. [33] and Chung et al. [22] are shown in Table 5. Fig. 8 and Table 5 show good agreement between experimental results and Eq. (1); although more studies are needed to verify these factors for different materials.

Endurance limit of structural member can be obtained from the laboratory determined endurance limit as [32]:

$$S_e = K_a K_b K_c K_d K_e S'_e \tag{3}$$

where S_e is endurance limit of structural member, S'_e is endurance limit of test specimen, K_a is surface factor, K_b is size factor, K_c is load factor, K_d is temperature factor and K_e is miscellaneous-effects factor. If ECAPed material used in the structure, the endurance limit would be:

$$S_e = K_a K_b K_c K_d K_e K_h S'_e \tag{4}$$

where K_h is defined by Eq. (1). The design application of Eq. (4) is that there is no need for lengthy fatigue test to obtain endurance limit for structure member made from ECAPed materials.

Table 4
The magnitudes of two modifying factors in endurance limit.

Material	K_h	K_l (1000 cycles)
Pure Al	2.69	2.38
Al6061	2.21	1.77
Pure Cu	2.25	4.7

Table 5
The fatigue endurance limit at (2×10^6) cycles.

	Material	$S_{ut}(CG)$ (MPa)	$S_{ut}(UFG)$ (MPa)	$\sigma_a(CG)$ (MPa) (experimental)	$\sigma_a(UFG)$ (MPa) (experimental)	σ_a (MPa) (Eq. (1))
Goto et al. [21]	Cu	232	402	49	72	84
Han et al. [33]	Cu	188	440	49	107	114
Chung et al. [22]	Al6061	273	420	60	85	92
Present work	Pure Al	62	167	24	57	64
	Al6061	122	270	55	111	121
	Cu	214	481	103	195	231

4. Conclusion

Commercial pure aluminum, aluminum 6061 alloy and commercial pure copper are pressed by route B_C using an ECAP die with the die channel angle of 90°. The prominent conclusions can be drawn as following:

- The average grain size of pure Al, Al6061 and pure Cu the ECAP process are approximately $(5–9) \times 10^{-3}$ times finer that initial alloys.
- The hardness magnitude of the ECAPed pure Al, Al6061 and pure Cu are 100–250% higher than un-ECAP alloys. More studies are needed to investigate the effect of more passes on the hardness value.
- Improvements of more than three times yield strength and more than twice in ultimate tensile strength are seen in ECAPed alloys in comparison with un-ECAPed alloys.
- The elongation of the alloys falls about 45–75% during the ECAP process.
- Two fatigue design factors obtained from uniaxial tension test has been proposed to correlate the endurance limit S_e UFG materials with endurance limit S'_e of the CG materials. Lengthy fatigue test to obtain endurance limit for structure member made from ECAPed materials can be avoided. Also, the endurance limit of the alloys increases drastically with applying ECAP operation.

References

[1] M. Furukawa, Y. Ma, Z. Horita, M. Nemoto, R.Z. Valiev, T.G. Langdon, Materials Science and Engineering A241 (1998) 122–128.
[2] V.M. Segal, Materials Science and Engineering A338 (2002) 331–344.
[3] R. Ding, C. Chung, Y. Chiu, P. Lyon, Materials Science and Engineering A 527 (2010) 3777–3784, doi:10.1016/j.msea.2010.02.030.
[4] T. Peng, Q.D. Wang, J.B. Lin, Materials Science and Engineering A 516 (2009) 23–30, doi:10.1016/j.msea.2009.04.024.
[5] G. Khatibi, J. Horky, B. Weiss, M.J. Zehetbauer, International Journal of Fatigue 32 (2010) 269–278, doi:10.1016/j.ijfatigue.2009.06.017.
[6] G. Krallics a, J.G. Lenard, Journal of Materials Processing Technology 152 (2004) 154–161, doi:10.1016/j.jmatprotec.2004.03.015.
[7] M. Kazeminezhad, E. Hosseini, Materials and Design 31 (2010) 94–103, doi:10.1016/j.matdes.2009.07.008.
[8] Y.G. Ko, D.H. Shin, K.-T. Park, C.S. Lee, Scripta Materialia 54 (2006) 1785–1789.
[9] V.V. Stolyarov, Y.T. Zhu, I.V. Alexandrov, T.C. Lowe, R.Z. Valiev, Materials Science and Engineering A299 (2001) 59–67.
[10] S. Xu, G. Zhao, Y. Luan, Y. Guan, Journal of Materials Processing Technology 176 (2006) 251–259, doi:10.1016/j.jmatprotec.2006.03.167.
[11] L.B. Tong, M.Y. Zheng, X.S. Hu, K. Wu, S.W. Xu, S. Kamado, Y. Kojima, Materials Science and Engineering A (2008), doi:10.1016/j.msea.2010.03.062.
[12] F. Djavanroodi, M. Ebrahimi, Materials Science and Engineering A 527 (2010) 1230–1235, doi:10.1016/j.msea.2009.09.052.
[13] S. Suresh, Fatigue of Materials, Cambridge University Press, 1991.
[14] H. Mughrabi, in: T.C. Lowe, R.Z. Valiev (Eds.), Investigations and Applications of Severe Plastic Deformation, 3/80, NATO Science Series, Kluwer Publishers, 2000, p. 241.
[15] H. Mughrabi, H.W. Höppe, M. Kautz, Scripta Mater 51 (2004) 807.
[16] A. Vinogradov, S. Agnew, in: J.A. Schwarz, C. Contescu, K. Putyera (Eds.), Dekker Encyclopedia of Nanoscience and Nanotechnology, Marcel Dekker Inc., USA, 2004, p. 2269.
[17] H.W. Hoppel, M. Kautz, H. Mughrabi, Proceedings of the 9th International Fatigue Conference, Elsevier, 2006, FT207.
[18] H. Mughrabi, H.-W. Höppel, A. Vinogradov, in: M.J. Zehetbauer, Y.T. Zhu (Eds.), Bulk Nanostructured Materials, Wiley–VCH, 2009.
[19] Y. Estrin, A. Vinogradov, International Journal of Fatigue 32 (2010) 898–907, doi:10.1016/j.ijfatigue.2009.06.022.
[20] C. Xu, Q. Wang, M. Zheng, J. Li, M. Huang, Q. Jia, J. Zhu, L. Kunz, M. Buksa, Materials Science and Engineering A 475 (2008) 249–256, doi:10.1016/j.msea.2007.04.074.
[21] M. Goto, S.Z. Han, K. Euh, J.-H. Kang, S.S. Kim, N. Kawagoishi, Scripta Materialia 58 (2010) 6294–6305.
[22] C.S. Chung, J.K. Kim, H.K. Kim, W.J. Kim, Materials Science and Engineering A337 (2002) 39–44.
[23] A. Vinogradov, Journal of Material Science 42 (2007) 1797–1808.
[24] M. Ferry, N. Burhan, Scripta Materialia 56 (2007) 525–528, doi:10.1016/j.scriptamat.2006.11.015.
[25] P.L. Sun, C.Y. Yu, P.W. Kao, C.P. Chang, Scripta Materialia 47 (2002) 377–381.
[26] M. Kawasaki, Z. Horita, T.G. Langdon, Materials Science and Engineering A 524 (2009) 143–150.
[27] A. Mishra, B.K. Kad, F. Gregori, M.A. Meyers, Acta Materialia 55 (2007) 13–28, doi:10.1016/j.actamat.2006.07.008.
[28] C. Xu, T.G. Langdon, Journal of Material Science 42 (2007) 1542–1550.
[29] T. Hanlon, E.D. Tabachnikova, S. Suresha, Fatigue behavior of nanocrystalline metals and alloys, International Journal of Fatigue 27 (2005) 1147–1158.
[30] S.M. Liu, Z.G. Wang, Fatigue properties of 8090 Al–Li alloy processed by equal-channel angular pressing, Scripta Materialia 48 (2003) 1421–1426.
[31] R.W. Landgraf, Achievement of high fatigue resistance in metals and alloys, ASTM STP 467 (1970) 3.
[32] J.E. Shigly, C.R. Mischke, Mechanical Engineering Design, 8th edition, McGraw-Hill, 2008.
[33] S.Z. Han, M. Goto, C. Lim, S.-H. Kim, S. Kim, Journal of Alloys and Compounds 483 (2009) 159–161, doi:10.1016/j.jallcom.2008.02.115.